NRC Publications Archive
Archives des publications du CNRC

Numerical simulations of propeller wake impacting on a strut
He, M.; Veitch, B.; Bose, N.; Colbourne, D. B.; Liu, P.

This publication could be one of several versions: author's original, accepted manuscript or the publisher's version. / La version de cette publication peut être l'une des suivantes : la version prépublication de l'auteur, la version acceptée du manuscrit ou la version de l'éditeur.

Publisher's version / Version de l'éditeur:

13th Annual Conference and Workshop on Computational Fluid Dynamics [Proceedings], 2005

Questions? Contact the NRC Publications Archive team at
PublicationsArchive-ArchivesPublications@nrc-cnrc.gc.ca. If you wish to email the authors directly, please see the first page of the publication for their contact information.

Vous avez des questions? Nous pouvons vous aider. Pour communiquer directement avec un auteur, consultez la première page de la revue dans laquelle son article a été publié afin de trouver ses coordonnées. Si vous n'arrivez pas à les repérer, communiquez avec nous à PublicationsArchive-ArchivesPublications@nrc-cnrc.gc.ca.

National Research Council Canada   Conseil national de recherches Canada

Canada

Numerical Simulations of a Propeller Wake Impacting

on a Strut

Moqin He[1], Brian Veitch[1], Neil Bose[1], Colbourne Bruce[2], and Pengfei Liu[2]

[1]*Faculty of Engineering and Applied Science, Memorial University of Newfoundland*
St. John's, NL, A1B 3X5, Canada

[2]*Institute for Ocean Technology, National Research Council Canada*
St. John's, NL, A1B 3T5, Canada

Email: moqinhe@engr.mun.ca

ABSTRACT

This paper introduces a newly developed Wake Impingement Model (WIM) that aims to simulate of the dynamic loads induced by a three dimensional, unsteady, and strong vortical propeller wake. Simulations of loads on an ice class, tractor type podded propeller in straight ahead motion are presented consisting of mean loads on the propeller and side force on the pod and strut. The side force fluctuations for three different advance coefficients have also been predicted. These simulations were carried out by using a panel code, PROPELLA, with or without WIM. Simulated results were compared with and without WIM and with experimental data. The comparison of the propeller open water characteristics of two simulated results shown there is almost no difference between predictions with and without WIM. It was found by comparing with experimental data that the simulations of the side force on the pod and strut with WIM successfully captured the fluctuation which was dominated by the component at the blade passing frequency, although this was at a reduced level compared with the measurements.

1. INTRODUCTION

The wake impingement phenomenon exists widely in the flow fields of hydrodynamic, aerodynamic, and turbine machinery. Examples include the wake of a propeller impacting on a rudder downstream [1], the wake from a canard encountering a wing of a fighter [2], and the wake of a rotator blade being cut by a vane of a stator [3]. Podded propellers, which are driven directly by motors housed and suspended under ship sterns by struts, have been receiving increasing interest from both industry and academics during the last decade. Applications are growing fast while the technology is still under development. In recognition of this, research work has focused on the propulsor design [4], performance optimization [5], and full scale extrapolation [6].

In spite of the above studies there has been little research on the dynamic load on the pod strut caused by propeller wake impingement. Deniset et al. [7] studied the steady and unsteady lift, drag, and moment on a pod by using a method based on the coupling between a potential flow code and a RANS code. Ohashi and Hino [8], and Sanchez-Caja and Pylkkanen [9] did similar studies for steady loads. Some numerical approaches are based on panel methods including different wake alignments and wake panel treatments [10, 11].

This study develops a 3D potential flow based wake impingement model for propeller wake/strut interaction. A validated panel code, PROPELLA [12], was used as the simulation platform. Starting with a relaxed and aligned wake emanating from the blade trailing edges, the motion of the wake sheet was traced step by step in time series. For each time step, every wake panel moves from the position at the previous step to a new location which was determined by the local induced velocity. When the wake approached the strut, a scheme was used to keep the wake panel from penetrating the body surface [13]. To avoid the large numerical disturbance resulting when two wake panels get too

close, the two dipole panels were merged before the calculation of the influence coefficients.

The rest of the paper is organized as follows. In section 2, we briefly describe the simulation method. In section 3, an ice class podded propeller, with experimental data for dynamic force comparisons, is described and simulation results are demonstrated. Comparisons with experimental data and discussions are made in section 4 followed by conclusions in section 5.

2. DESCRIPTION OF THE METHOD

The method is based on a low order panel code, PROPELLA. In order to simulate the blade wake responses to their impact with the pod and strut, a Wake Impingement Model (WIM) was developed to substitute the original wake alignment subroutine. The WIM includes a kinematical conditions part and a dynamic conditions part. The former part consists of schemes for tracing the wake panel positions, detecting penetrating wake panels and penetrated body panels, and diverting the penetrating wake panels to slip over the body surface. The second part includes schemes for merging wake strengths when two or more elements get close, and updating wake strengths after they were deformed by the interaction with the body. These schemes are described in following subsections.

2.1 Kinematical Condition of WIM

The implementation of the kinematical condition for wake impingement started from tracing the wake panels once they shed from the blade trailing edges. Each wake panel was geometrically represented by the four corners, and the combination of the four corners was traced step by step. For each time step, the locations of the wake shed at the present time step were defined by the trajectory of the blade trailing edge while other wake panels shed in previous time steps were marched to their new locations. The marching distance was the product of the time interval and the induced velocity

$$\vec{r}_{t+\Delta t} = \vec{r}_t + \vec{V}_t \Delta t \qquad (1)$$

where $\vec{V}_t$ is the induced velocity at the wake corner at time t, and Δt is the time interval. $\vec{r}_t$ is the wake corner position at time t, and $\vec{r}_{t+\Delta t}$ is the wake corner position at time $t + \Delta t$.

The wake positions predicted by Eq. (1) remain correct until some of them are predicted to go inside

or through the body. To prevent this, a detective scheme was performed following each step of the wake marching. The detective scheme scans all wake panels and all body panels for the impacting wake panels and impacted body panels. Once the impacting and impacted panels had been found, impacting wake panels were diverted to slip over the body surface at the corresponding impacted panels. The body boundary is defined as an enclosed surface as $S(x, y, z) = 0$, which can be represented by a number of body panels, m_{body}. They are expressed as

$$\{S_k(x, y, z) = 0, \quad k = 1,2, \quad m_{body}\} \qquad (2)$$

Once a wake corner, $\vec{r}_{t+\Delta t}$, was predicted to penetrate the body panel, $S_k(x, y, z) = 0$, the new wake corner position, as shown in figure 1, predicted by Eq. (1) was corrected by the following equation:

$$\vec{r}_{t+\Delta t} = \vec{r}_t + |\vec{V}_t| \Delta t \cdot \vec{l} \qquad (3)$$

where $\vec{l}$ is the unit vector tangential to the body surface measured from the wake panel corner. This scheme for detecting penetration and diverting the wake is applicable to cases of vortex particle/body interactions. For cases of quadrilateral wake panel/body interactions, the scheme involves a number of treatments to the combinations of four corners with different impacting status. Details about the treatments can be found in reference [13].
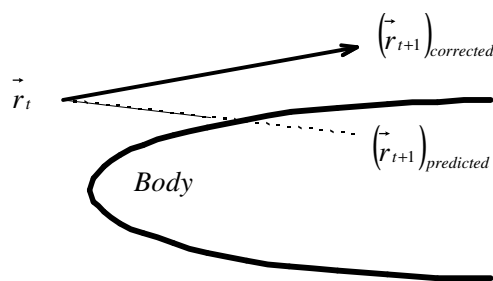

Figure 1 Non Penetration Correction

When a dipole panel or a vortex ring approaches a body surface, a large numerical disturbance will be raised in the induced velocity calculation. To avoid this disturbance, a "friendly distance" [11] was applied to keep all wake panels away from the body surface with a minimum allowable distance. The value of the friendly distance was chosen as a half of the estimated boundary layer thickness at the blade trailing edge. It was set in the range of 0.01 to 0.03 of the diameter of the propeller in simulations.

Similar to a vortex approaching a body, numerical disturbances might also be raised when two vortex

elements get close enough. When the distance between two wake panels was detected to be too small, the older wake panel was merged to the younger wake panel. The age of the wake was determined by the time since it was shed.

2.2 Dynamic Condition of WIM

The dynamic condition of the WIM includes the merger of the vortex strengths of two or more vortex elements, and the vortex transfer between an impacting wake panel and the corresponding impacted body panel. The main principle to follow is conserving the total vortex strength.

When two wake panels got too close to avoid a numerical disturbance in the induced velocity calculation, the two wake panels were merged. The vortex strength of the older wake panel was assigned to zero after its strength was transferred to the younger panel and the two panels were completely overlapped.

Through an investigation and simulation on a normal vortex-cylinder interaction in a viscous fluid, Gossler and Marshall [15] and Marshall and Krishnamoorthy [16] found that when an incident vortex approaches the cylinder, the vortex attached on the body ejects outward from the cylinder, forming secondary vortices, then wraps around and joins with the incident vortex. This phenomenon could happen during the impact of a blade wake on the strut and it was considered and modeled by a correction to the vortex strengths.

$$
\begin{aligned}
\left(\vec{\omega}_{t+\Delta t}\right)_{incident} &= \left(\vec{\omega}_{t}\right)_{incident} + \left(\vec{\omega}_{t}\right)_{imp} k_{2} \\
\left(\vec{\omega}_{t+\Delta t}\right)_{imp} &= (1-k_{2}) \times \left(\vec{\omega}_{t}\right)_{imp}
\end{aligned}
\tag{4}
$$

here $\left(\vec{\omega}_{t+\Delta t}\right)_{incident}$ and $\left(\vec{\omega}_{t}\right)_{incident}$ are the incident (blade wake) vortex strengths at time t and $t+\Delta t$ respectively, and $\left(\vec{\omega}_{t+\Delta t}\right)_{imp}$ and $\left(\vec{\omega}_{t}\right)_{imp}$ are the vortex strengths attached to the body panel which the incident vortex encounters. k_{2} is a factor to be determined by numerical tests. These vortex strengths on wake panels are determined by interpolations of the strengths on the panel sides. The strengths of vortex filaments $\gamma_{\xi}(\xi,\eta)$ and $\gamma_{\xi}(\xi,\eta)$ on the panel sides are calculated by equations [17].

$$
\begin{pmatrix} \gamma_{\xi}(\xi,\eta) \\ \gamma_{\eta}(\xi,\eta) \\ \gamma_{\zeta}(\xi,\eta) \end{pmatrix} = \begin{pmatrix} (\partial \mu / \partial \eta) \\ -(\partial \mu / \partial \xi) \\ 0 \end{pmatrix}
\tag{5}
$$

3. SIMULATIONS

An ice class podded propeller was chosen for the numerical simulations. The model propulsor was designed as an ice propeller dynamometer with measurements of forces and moments on the key blade, the propeller shaft and the whole unit. The propeller has four blades, the diameter is 0.3 meter, and the pitch ratio is 0.757. Details about the design and the geometry are described in reference [14]. The experimental data used for comparisons were collected under the operation conditions of 5, 7, 10 rps and 0.2, 0.5, and 0.8 m/s respectively. The sampling rate for each channel was 5 kHz. The propulsor was panelized as shown in Figure 2. The axis of x is along the propeller shaft, z is along the strut spanwise, upward positive, and y is starboard positive. Comparisons between simulations and experimental data include blade wake, open water characteristics and the fluctuations of the side force on the strut and pod.
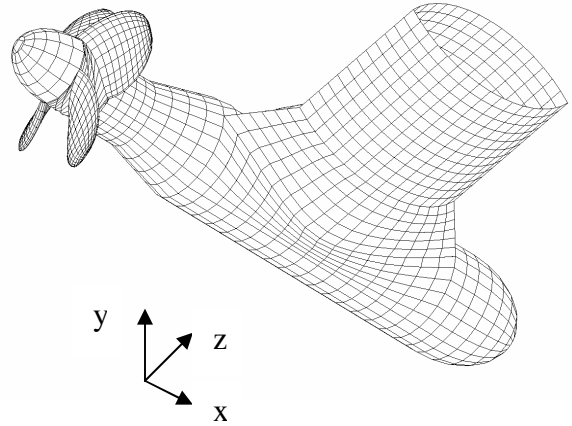

Figure 2 Panelized Propulsor

4. RESULTS AND DISCUSSION

In this section, the simulated blade wake with WIM is compared with that obtained without using the WIM by the same panel code. The calculated open water characteristics are compared with each other as well as with the experimental data. Comparisons and discussions on the fluctuation of the side force on the strut and pod are also made in this section.

4.1 Effect on the Blade Wake

For most potential flow based lifting surface methods, the deformation of the blade wake due to wake impingement is not considered. Therefore, the wake geometry after the collision with a body in the

propeller race might have not been realistically presented and some hydrodynamic properties, such as the pressure and force fluctuations on the afterbody might not be accurately predicted. When they are applied to a tractor type podded propeller, the influence by the part of blade wake that originally goes through the pod and strut as shown in Figure 3 have been cancelled in the work of reference [10] or artificially reduced in the work of reference [11]. The wake simulated by the panel code with WIM is shown in Figure 4. The wake panels having a tendency to go through the body surface have been diverted to pass around the body. A continuous helical wake sheet has been cut into pieces forming a set of spring washer shaped wake sheets after it passes the strut. The results with the WIM appear to be more realistic.
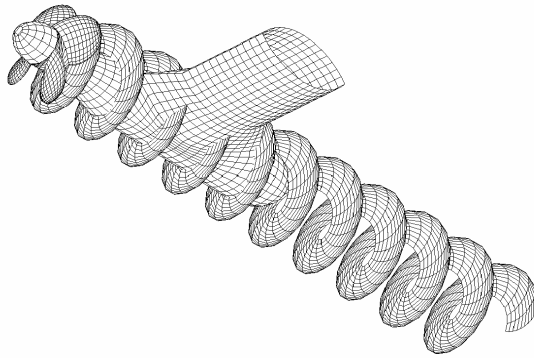

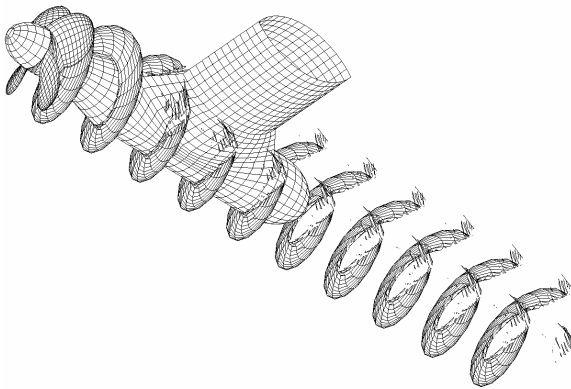Figure 3 Propeller Wake without WIM

Figure 4 Propeller Wake with WIM

4.2 Effect on Propeller Characteristics

The simulated open water characteristics with and without the WIM are shown in Figure 5. The thrust and torque coefficients, K_t and K_q, are defined as

$$K_t = T / \left(\rho n^2 D^4 \right) \tag{6}$$

and

$$K_q = Q / \left(\rho n^2 D^5 \right) \tag{7}$$

Here T and Q are the thrust and torque of the propeller, ρ is the water density, n is the rotation speed, and D is the diameter of the propeller. Comparisons of thrust and torque coefficients, K_t and K_q, show that there is almost no difference between simulations with and without the WIM. This implies the WIM has no effect on the propeller performance prediction by the original panel code, PROPELLA. Compared to the experimental data both calculated thrust coefficients with and without using the WIM are higher. Predictions on the torque coefficient are very close to the test result except in the range of the extreme low advance coefficient, $J < 0.25$.
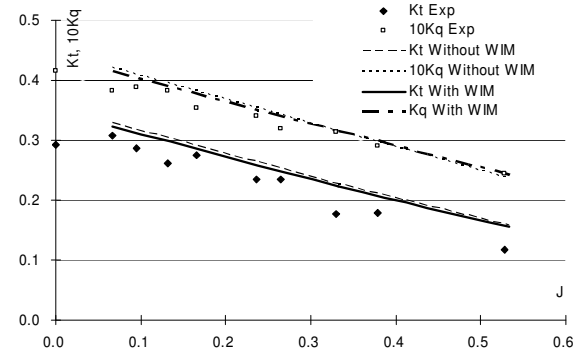

Figure 5 Open Water Characteristics

4.3 Effect on Dynamic Force on Strut

Since the panel code deals with viscous terms only by empirical corrections and the experimental data are unable to exclude the viscous effects, comparisons of the global forces dominated by viscous terms would contribute little to the validation of the simulation method with WIM. Comparisons of dynamic forces in this section are focused on the components that are significantly affected by the blade passing frequency. The side force Y is defined the total force on the strut and the pod in the direction of the axis of y as shown in Figure 2. Based on the investigation of the measured fluctuations of global forces, the side force Y was found being dominated by the component of the blade passing frequency. This implies that Y is one of the most sensitive global forces to the wake impingement. The comparisons for three different

advance coefficients are shown in Figure 6 to 8. Both numerical and experimental results shown in the figures indicate the side force coefficient, $K_y = Y/(\rho n^2 D^4)$, changes with the advance speed very slightly.

From Figure 6 to 8, one can see that with the advance coefficient increasing from 0.13 to 0.53, the mean of measured K_y drops from 0.087 to 0.071 and the amplitude of the fluctuation component of the blade passing frequency decreases from 0.092 to 0.077. The variations of the side force were dominated by the frequency of four times, the number of blades, of the revolution speed of the propeller. Compared with
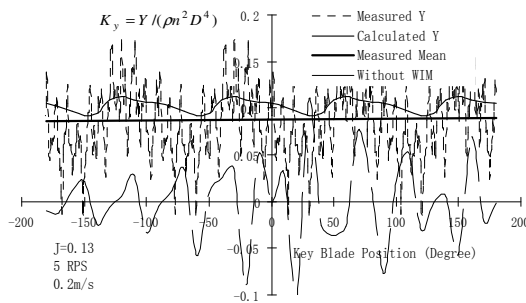

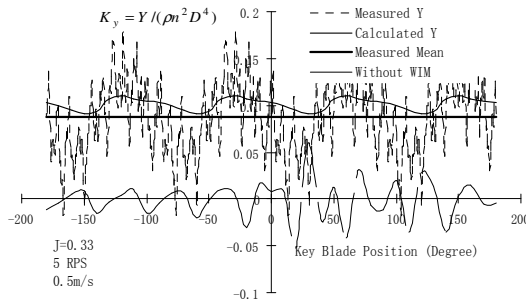Figure 6 Dynamic Side Force Y (J=0.13)

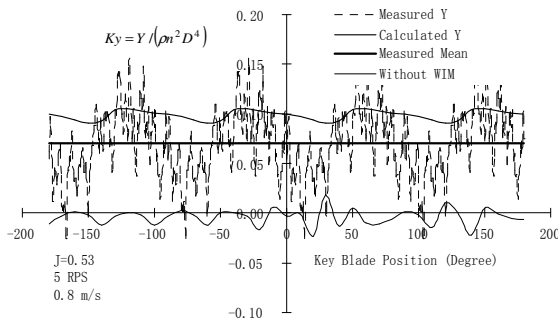Figure 7 Dynamic Side Force Y (J=0.33)

Figure 8 Dynamic Side Force Y (J=0.53)

the measurements the fluctuation component of the blade passing frequency was successfully captured by the simulations with WIM. However, the amplitude of the component was lower than that from the measurements. Simulations with WIM on means of all three J are a little higher than that from experiments. The simulated means without using WIM did not change with the advance coefficient and all of them for three different J are very close to zero. The reason might be due to the cancellation of the influence from the blade wake located from the foremost to the aftermost part of the pod.

5. CONCLUSION

A wake impingement model has been developed, inserted in a panel code and applied to an ice class podded propeller. Simulations and comparisons with experimental data show that with the wake impingement model the prediction of propeller blade wake is more realistic when there is a body in the race of the wake. The wake impingement model does not affect the prediction of the propeller performance by the original code, and it improves the simulation in capturing the fluctuation component of the blade passing frequency of the side force on the strut and pod.

REFERENCES

[1]. Molland AF, and Turnock SR. Wind Tunnel Investigation of the Influence of Propeller Loading on Ship Rudder Performance. *Transactions of the Royal Institution of Naval Architects.* 1993;135:105-120.
[2]. Mahalingam R, Funk RB, and Komerath NM. *Low Speed Canard-Tip-Vortex Airfoil Interaction.* Wichita, KS: SAE General, Corporate, and Regional Aviation Meeting and Exposition; April 1997. SAE Paper No. 971469.
[3]. Ren Y, Toshinori W, Shojiro K. Numerical Simulation of Rotator-stator Interactions in a Transonic Compressor Stage. *Tsinhua Science and Technology.* 2000; 5, 1: 76-81,88.
[4]. Bushkovsky VA, Frolova I, Kaprantsev SV, Pustoshny AV, Vasiljev AV and Jacolev AJ. *On the*

design of a shafted propeller plus electric thruster contra-rotating propulsion complex. University of Newcastle, UK: First International Conference on Technological Advances in Podded Propulsion; 14-16 April 2004.

[5]. Bertaglia G, Lavini G and Scarpa S. *Hull design and optimization with pod propellers with 5 and 6 blades.* University of Newcastle, UK: First International Conference on Technological Advances in Podded Propulsion; 14-16 April 2004.

[6]. Chicherin IA, Lobatchev M, Pustoshny AV and Sanchez-Caja A. *On a propulsion prediction procedure for ships with podded propulsors using RANS-code analysis.* University of Newcastle, UK: First International Conference on Technological Advances in Podded Propulsion; 14-16 April 2004.

[7]. Francois Deniset, Jean-Marc Laurens and Rachel Jaouen. *Numerical Simulations of Podded Propulsors.* Rome, Italy: 6th Numerical Towing Tank Symposium; 29 September – 1 October, 2003.

[8]. Kunihide Ohashi, Takanori Hino, and Yoshitaka Ukon. *Flow Computations of a Ship with a Podded Propulsor.* Rome, Italy: 6th Numerical Towing Tank Symposium; 29 September – 1 October, 2003.

[9]. Antonio Sanchez_Caja and Jaakko V. Pylkkanen. *On the hydrodynamic design of Podded propulsors for fast commercial vessels.* University of Newcastle, UK: First International Conference on Technological Advances in Podded Propulsion; 14-16 April 2004.

[10]. Liu P and Bose N. Hydrodynamic characteristics of a screw-nozzle-rudder assembly. *Computational Fluid Dynamics Journal of Japan,* 2001; Special Number: 477-484.

[11]. Chen SH and Williams MH. A panel method for counter rotating profanes, AIAA, Inc. 1987.

[12]. Liu P and Bose N. *An Unsteady Panel Method for Highly Skewed Propeller in Non-Uniform Inflow.* Grenoble, France: 22nd ITTC Propulsion Committee Propeller RANS/Panel Method Workshop; 1998.

[13]. He M, Veitch B, Bose N, Colbourne B and Liu P. *A Three Dimensional Wake Impingement Model and Applications on Tandem Oscillating Foils.* under review

[14]. Bell J. Podded propellers in ice apparatus design. Institute for Ocean Technology, NRC: Report No. LM-2003-028

[15]. Gossler AA and Marshall JS. Simulation of normal vortex-cylinder interaction in a viscous fluid. *Journal of Fluid Mechanics.* 2001; 431: 371-405.

[16]. Marshall JS, and Krishnamoorthy S. On the instantaneous cutting of a columnar vortex with non-zero axial flow. *Journal of Fluid Mechanics.* 1997; 351: 41-74.

[17]. Hess JL. Calculation of Potential Flow about Arbitrary Three–Dimensional Lifting Bodies. AD-755 480, Appendix A